Synthesis, Characterization, and Catalytic Applications of Manganese Oxide Octahedral Molecular Sieve (OMS) Nanowires with a 2 × 3 Tunnel Structure

Xiongfei Shen,[†] Yunshuang Ding,[†] Jia Liu,[‡] Kate Laubernds,[§] Richard P. Zerger,[∥] Mihai Polverejan,[⊥] Young-Chan Son,[⊥] Mark Aindow,[#] and Steven L. Suib*[,†,⊥]

Institute of Materials Science, Department of Chemistry, and Department of Metallurgy and Materials Engineering, University of Connecticut, Storrs, Connecticut, 06269

Received May 4, 2004. Revised Manuscript Received July 27, 2004

Romanechite is a natural manganese oxide with a 2 × 3 tunnel structure containing a majority of Ba^{2+} and trace amounts of Na^+, K^+, and Sr^{2+} as tunnel cations. Many attempts have been made to synthesize the 2 × 3 tunnel structured manganese oxide in laboratories using Ba^{2+} as the template. However, no successful work has been reported due to (1) the presence of intergrown hollandite impurities (barium-2 × 2 tunnel structure manganese oxide) in the synthesized products and (2) the absence of romanechite characteristic X-ray diffraction (XRD) peaks in the products, such as the (001) and (200) diffraction peaks which correspond to $d \approx 9.7$ and 7.0 Å, respectively. Hydrated Na^+ ions have been utilized as structure directors to successfully synthesize the Na-2 × 3 tunnel structure manganese oxide (OMS-6) from hydrothermal treatment of Na-birnessite. XRD gave a pattern in very good agreement with the pattern of romanechite (JCPDS file 14-627) without impurity phases. High-resolution microscopy measurements showed a nanofibrous morphology of the materials with an average fiber diameter of 40 nm. Under N_2 environments, the 2 × 3 tunnel structure is stable below 550 °C and transforms into hausmannite (Mn_3O_4) at temperatures of 550 °C or higher; however, under O_2 environments, the 2 × 3 tunnel structure is preserved at 550 °C as measured by in situ XRD. The density functional theory (DFT) method indicated that the 2 × 3 tunnel structure has a major micropore size of 7.5 Å. NH_3 and CO_2 chemisorption results indicated that the amount of strong acidic and basic sites on the Na-2 × 3 material is about 0.22 and 0.002 mmol/g sample, respectively. Catalytic oxidation of indene by the Na-2 × 3 manganese oxide showed a 96% conversion for indene and a 73% selectivity toward phthalic anhydride for a 40 h reaction at 80 °C.

1. Introduction

Manganese oxides are one of the largest families of porous materials with various structures as found in manganese oxide minerals all over the world. Among them are two major structures: (1) layered materials constructed by edge sharing of MnO_6 octahedra to form sheets with cations such as Na^+ and K^+ and one layer or two layers of H_2O present between any two adjacent sheets; and (2) tunnel structures constructed by both edge and corner sharing of MnO_6 octahedra to form 1 × 1 tunnels (Pyrolusite), 1 × 2 tunnels (Ramsdellite), 1 × 1/1 × 2 inter-grown tunnels (Nustite), 2 × 2 tunnels (Hollandite or Cryptomelane with Ba^{2+} or K^+ in the tunnel, respectively), 2 × 3 tunnels (Romanechite), or 3 × 3 tunnels (Todorokite).[1−4]

This diversity of manganese oxides in atomic architectures and structures will, in turn, result in diversity of manganese oxides in chemical properties and activities for potential applications such as cation-exchange, ion and molecule separation, chemical sensor, battery, catalysis, and patterning. Therefore, there has been tremendous research interest in laboratory synthesis of manganese oxides to reproduce the structures of natural manganese oxides or produce new ones.[5−10]

For instance, based on the work of Golden,[11] by hydrothermal treatment of Mg-layered manganese oxide

* Corresponding author. E-mail: suib@uconnvm.uconn.edu. Tel: (860) 486-2797. Fax: (860) 486-2981.
[†] Institute of Materials Science.
[‡] Current address: Institute for Lasers, Photonics and Biophotonics, The State University of New York at Buffalo, Buffalo, NY, 14260.
[§] Current address: Naval Air Systems Command, Patuxent River, MD, 20670.
[∥] Current address: 300 East 27th Street, North Newton, Kansas, 67117.
[⊥] Department of Chemistry.
[#] Department of Metallurgy and Materials Engineering.

(1) Bish, D. L.; Post, J. E. *Am. Mineral.* **1989**, *74*, 177.
(2) Brock, S. L.; Duan, N. G.; Tian, Z. R.; Giradlo, O.; Zhou, H.; Suib, S. L. *Chem. Mater.* **1998**, *10*, 2619.
(3) Feng, Q.; Kanoh, H.; Ooi, K. *J. Mater. Chem.* **1998**, *9*, 319.
(4) Post, J. E. *Proc. Natl. Acad. Sci. U.S.A.* **1999**, *96*, 3447.
(5) Golden, D. C.; Dixon, J. B.; Chen, C. C. *Clays Clay Miner.* **1986**, *34*, 511.
(6) Tian, Z. R.; Tong, W.; Wang, J. Y.; Duan, N. G.; Krishnan, V. V.; Suib, S. L. *Science* **1997**, *276*, 926.
(7) Brock, S. L.; Duan, N. G.; Tian, Z. R.; Giraldo, O.; Zhou, H.; Suib, S. L. *Chem. Mater.* **1998**, *10*, 2619.
(8) Tsuda, M.; Arai, H.; Nemoto, Y.; Sakurai, Y. *J. Power Sources* **2001**, *102*, 135.
(9) Djurfors, B.; Broughton, J. N.; Brett, M. J. *J. Mater. Sci.* **2003**, *38*, 4817.
(10) Giraldo, O.; Brock, S. L.; Marquez, M.; Suib, S. L.; Hillhouse, H.; Tspatsis, M. *Nature* **2000**, *405*, 38.
(11) Golden, D. C.; Chen, C. C.; Dixon, J. B. *Science* **1986**, *231*, 717.

10.1021/cm049291r CCC: $27.50
Published on Web 11/16/2004

at 150−180 °C for 2 d, Shen successfully synthesized a 3 × 3 tunnel structure manganese oxide corresponding to natural todorokite (3 × 3 tunnel structure).[12] The obtained 3 × 3 octahedral molecular sieve (OMS-1) is thermally stable up to 600 °C and comparable to natural todorokite (~500 °C). Different metal ions (M) with similar ionic radii and charges as Mg^{2+} (such as M = Co^{2+}, Ni^{2+}, Cu^{2+}, and Zn^{2+}) were also used as templates to synthesize M-OMS-1 with a 3 × 3 tunnel structure.[13]

Manganese oxide with a 2 × 2 tunnel structure (OMS-2) corresponding to natural cryptomelane was synthesized by refluxing $KMnO_4$ and Mn^{2+} solutions with concentrated HNO_3 at 100 °C for 24 h.[14] Molecular modification to generate metal-doped OMS-2 can be achieved by refluxing $KMnO_4$ and Mn^{2+} solutions with metal ions[15] or conducting high-temperature (~800 °C) calcination of Fe-doped K-birnessite[16] or calcination of $KMnO_4$, $Mn(NO_3)_2$, KNO_3, and $Fe(NO_3)_3$ with cross-linking reagents.[17]

A new 2 × 5 tunnel structure manganese oxide ($Rb_{0.27}MnO_2$), which is seldom found in nature, was synthesized by Yamamoto from hydrothermal treatment of β-MnO_2 with RbOH solution in a gold capsule at 350 °C and 200 MPa for 48 h.[18] Another manganese oxide with a new 2 × 4 tunnel structure (RUB-7) was synthesized by Rziha from hydrothermal treatment of synthetic Rb-birnessite with RbOH solution at 350 °C in a gold capsule for 2 d.[19] The Na-2 × 4 tunnel structure was also synthesized by Xia[20] by autoclaving Na-birnessite with 5 M NaCl at 180−240 °C for 2 d and by Liu[21] via autoclaving Na-birnessite with 2 M NaOH at 150 °C for 10 d. Recently, the Na-2 × 4 tunnel structure was obtained by autoclaving Na-birnessite with 1 M NaOH at 180 °C within 2 d.[22]

Romanechite is a natural manganese oxide with a 2 × 3 tunnel structure, which has a relatively large tunnel size similar to that of alumino-silicate zeolites. As shown in the work on OMS-1, OMS-2, and 2 × 4 tunnel structure manganese oxides, once the structure can be reproducibly synthesized in laboratories, structural modification or molecular decoration can be performed to generate a wider variety of functional materials. Therefore, many attempts have been made to produce synthetic manganese oxides having a 2 × 3 tunnel structure like that of natural romanechite.

Based on the initial structure work on romanechite by Wadsley,[23,24] Burner[25] refined the structure of natural romanechite indicating that it is monoclinic having a space group of $C2/m$ with $a = 13.93$ Å, $b = 2.846$ Å, $c = 9.678$ Å, and $\beta = 92.39°$. The formula of romanechite is $(Ba,H_2O)_2Mn_{10}O_{20}$ with a majority of Ba^{2+} and trace amount of Na^+, K^+, and Sr^{2+} cations present in the tunnel. Since Ba^{2+} is the major cation in the tunnel of romanechite, Ba-layered manganese oxide has been widely tried as the template for synthesis of 2 × 3 tunnel structure manganese oxide.[26−29] Wadsley reported the synthesis of psilomelane, which was referred to as romanechite at that time, from hydrothermal treatment of $(Ba,Mn)Mn_3O_7 \cdot nH_2O$ with $BaCl_2$ at 160 °C for several weeks.[26] However, compared to natural romanechite, which has a maximum d spacing of about 9.7 Å for the (001) planes, the synthesized material had a largest d spacing of 9.1 Å which indicates that the synthesized material is not exactly the 2 × 3 tunnel structure manganese oxide.

Giovanoli also tried the synthesis of romanechite by autoclaving of Ba-phyllomanganate with $BaCl_2$ at 600 °C under 2 kbar.[26] However, hollandite (barium-2 × 2 tunnel structure) and unidentified impurity particles were clearly observed by TEM. Feng and Tsuda reported the synthesis of romanechite from hydrothermal treatment of Ba-birnessite with 0.5 M $BaCl_2$ at 180 °C for 2 d.[28,29] However, the presence of Mn_3O_4 impurities and the absence of the characteristic diffraction peaks for the (001) planes makes this questionable.

Therefore, the synthesis of romanechite in laboratories has always been questionable either due to (1) the presence of hollandite impurities, which very readily intergrow with romanechite as observed by Buseck,[30] or Mn_3O_4 impurities; or (2) the absence of the characteristic diffraction peak for the (001) planes which corresponds to $d \approx 9.7$ Å, the spacing of the 3 MnO_6 chain in the 2 × 3 tunnels. Here, we report the synthesis of the 2 × 3 tunnel structure manganese oxide using hydrated Na^+ ions as the structure director by hydrothermal treatment of Na-birnessite itself at 200−250 °C for 2 d. The synthesized Na-2 × 3 tunnel structure clearly shows characteristic diffraction for the (001) planes of romanechite with the whole XRD pattern in very good agreement with natural romanechite.

2. Experimental Section

2.1 Material Preparation. Sodium birnessite was first prepared by the redox method as reported in the literature.[20,31] In a typical experiment, 6.32 g (0.04 mol) of $KMnO_4$ and 48 g (1.2 mol) of NaOH were dissolved in 400 mL of DDW to prepare solution A; then 22.48 g (0.112 mol) of $MnCl_2 \cdot 4H_2O$ was dissolved in 400 mL of DDW to prepare solution B. Solution B was added dropwise into solution A with vigorous stirring in an ice bath. The resultant black precipitate was statically aged at room temperature for 1 d and then washed and dried. The yield of the dried birnessite is about 15 g. About 0.5 g of dried Na-birnessite precursor was dispersed into 15 mL of DDW in a 23-mL Teflon liner and autoclaved at 200−240 °C for 2 d to obtain the final product, sodium 2 × 3 tunnel structure manganese oxide.

(12) Shen, Y. F.; Zerger, R. P.; DeGuzman, R. N.; Suib, S. L.; McCurdy, L.; Potter, D. I.; O'Young, C. L. *Science* **1993**, *260*, 511.
(13) Shen, Y. F.; Suib, S. L.; O'Young, C. L. *J. Am. Chem. Soc.* **1994**, *116*, 11020.
(14) DeGuzman, R. N.; Shen, Y. F.; Neth, E. J.; Suib, S. L.; O'Young, C. L.; Levine, S.; Newman, J. M. *Chem. Mater.* **1994**, *6*, 815.
(15) Chen, X.; Shen, Y. F.; Suib, S. L.; O'Young, C. L. *J. Catal.* **2001**, *197*, 292.
(16) Cai, J.; Liu, J.; Willis, W. S.; Suib, S. L. *Chem. Mater.* **2001**, *13*, 2413.
(17) Liu, J.; Song, Y. C.; Cai, J.; Shen, X. F.; Suib, S. L.; Aindow, M. *Chem. Mater.* **2004**, *16*, 276.
(18) Yamamoto, N.; Tamada, O. *J. Cryst. Growth* **1985**, *73*, 199.
(19) Rziha, T.; Gies, H.; Rius, J. *Eur. J. Mineral.* **1996**, *8*, 675.
(20) Xia, G. G.; Tong, W.; Tolentino, E. N.; Duan, N. G.; Brock, S. L.; Wang, J. Y.; Suib, S. L. *Chem. Mater.* **2001**, *13*, 1585.
(21) Liu, Z. H.; Ooi, K. *Chem. Mater.* **2003**, *12*, 3696.
(22) Shen, X.; Ding, Y.; Suib, S. L. Unpublished results.
(23) Wadsley, A. D. *Nature* **1952**, *170*, 4336.
(24) Wadsley, A. D. *Acta Crystallogr.* **1953**, *6*, 433.
(25) Turner, S.; Post, J. E. *Am. Mineral.* **1988**, *73*, 1155.
(26) Wadsley, A. D. *Am. Mineral.* **1950**, *35*, 485.
(27) Giovanoli, R.; Balmer, B. *Chimica* **1983**, *37*, 424.
(28) Feng, Q.; Yanagisawa, K.; Yamasaki, N. *J. Porous Mater.* **1998**, *5*, 153.
(29) Tsuda, M.; Arai, H.; Nemoto, Y.; Sakurai, Y. *J. Power Sources* **2001**, *102*, 135.
(30) Buseck, P. R. *Science* **1979**, *203*, 456.
(31) Luo, J.; Huang, A.; Park, S. H.; Suib, S. L.; O'Young, C. L. *Chem. Mater.* **1998**, *10*, 1561.

2.2 Characterization. *Structure.* The structure of the prepared materials was first analyzed with XRD using a Scintag PDS 2000 diffractometer with a Cu Kα X-ray source in a step scan mode with a scan rate of 2 s/step and a step size of 0.01° (2θ). The materials then were further investigated by high-resolution transmission electron microscopy (HRTEM). HRTEM images were obtained in a JEOL 2010 FasTEM operating at 200 kV. This instrument is equipped with a high-resolution objective lens pole-piece (Cs = 0.5 mm) giving a point-to-point resolution of <0.19 nm in phase contrast images. TEM sample preparation was performed by dispersing the specimen in N-butanol, dropping the solution onto a holey carbon coated 300-mesh copper grid (SPI), and allowing the butanol to evaporate.

Morphology. Morphology of the material was analyzed with a Zeiss DSM 982 Gemini field emission scanning electron microscopy (FESEM). Powder specimens were dispersed in acetone, dropped onto a gold-coated silicon wafer, and then the dried wafer was mounted onto a stainless steel sample holder.

Thermal Stability. Thermal stability of the materials was studied with thermogravimetric analysis (TGA), temperature-programmed desorption (TPD), and in situ XRD measurements. TGA measurements were conducted in a Hi-Res TGA 2950 thermogravimetric analyzer with 60 mL/min of N_2 flow from 25 to 700 °C with a heating rate of 20 °C/min.

TPD was performed in a homemade setup equipped with a MSS-RGA mass spectroscopy detector (MKS instruments). About 50 mg of the sample was first degassed in 40 mL/min of He flow overnight and then was heated under 40 mL/min of He flow at a heating rate of 2 °C/min from 25 to 125 °C and 1 °C/min from 125 to 725 °C.

Structural changes of the 2 × 3 tunnel structure with temperature were investigated with in situ XRD under N_2 or O_2 environments in an Xtra-50 in situ X-ray diffractometer (Thermo ARL). XRD patterns were recorded after the material was held at experimental temperatures (RT, 150 °C, and 550 °C) for 2 h using the same step scan mode as that used in the conventional XRD measurements.

Chemical Composition. Elemental composition of the materials was analyzed with inductively coupled plasma−optical emission spectroscopy (ICP−OES), a Perkin-Elmer Optima 3300XL spectrometer, combined with TPD measurement results, and titration of the average oxidation state (AOS) of framework manganese. Samples were dissolved in concentrated HCl to prepare a solution of manganese oxide with a concentration of about 500 mg/L for ICP−OES measurements. AOS titrations were conducted using the method described in the literature.[16,20]

Surface Area and Porosity. N_2 physisorption was performed in a Micromeritics ASAP 2010 instrument to study surface area, pore volume, and pore size distribution of the materials. Samples were pretreated by degassing at 300 °C for about 10 h to remove any adsorbed species and tunnel water. An incremental dosage mode with a dosing rate of 0.1 cm^3/g was used to measure microporosity under low-pressure ranges. A nonlocal density functional theory (NLDFT) method for the slit-pore geometry was used to extract microporosity and adsorptive energy distributions using the procedures suggested by Olivier and Occelli.[32,33] The NLDFT method is included in the DFT Plus software package as provided by Micromeritics. When the pores are immersed in a single component fluid (adsorptive such as N_2) at a fixed temperature and pressure, the fluid will diffuse to the pore walls and reach an equilibrium distribution. At equilibrium conditions, the chemical potential at every point is equal to the chemical potential of the bulk fluid. The bulk fluid is a homogeneous system of constant density and its chemical potential is determined by the pressure of the system. However, the fluid near the pore walls is not of constant density; its chemical potential is composed of several position-dependent contributions that must total at every point to the same value as the chemical potential of the bulk fluid. In addition, at equilibrium, the whole system has a minimum free energy, which is known thermodynamically as the grand potential energy (GPE). DFT describes the thermodynamic GPE as a functional of the single-particle density distribution. Therefore, calculating the density profile that minimizes the GPE will yield the equilibrium density profile. Then the equilibrium density profiles for different pore sizes can be used to construct models to describe the adsorption isotherm. The models then can be used for extracting pore size distributions of unknown samples. This is the general way that the DFT method is used for extracting pore size distributions.

From DFT, the total adsorption of adsorbate at every pressure can also be expressed as the convolution of a distribution of adsorbate−adsorbent (fluid−solid) interaction intensity, which is determined by the interaction energy. The integral operation of this adsorbate−adsorbent interaction intensity will produce the adsorption isotherm. As a result, model isotherms can be constructed from a wide range of adsorptive energies. Experimental data then can be fitted into the models to extract distributions of surface adsorptive energy. More complete theoretical work about how to apply DFT to extract pore size distributions and surface adsorptive energy distributions can be found in the literature.[32−34]

Strong Acidic and Basic Sites. NH_3 and CO_2 chemisorption measurements were also conducted in the Micromeritics ASAP 2010 instrument to analyze the amount of strong acidic and basic sites in the materials. About 1.5 g of the fresh material was first evacuated at 125 °C for 2 h to remove the adsorbed species followed by adsorption measurements at RT (~25 °C) at gas pressures from 100 to 700 Torr. After the first adsorption measurement, the material was evacuated at the analysis temperature (25 °C) for 1 h, and then a second adsorption was measured. The first measurement produces the total amount of gas adsorption resulting from physisorption, weak chemisorption, and strong chemisorption. The second measurement produces the amount of adsorption resulting from physisorption and weak chemisorption. Therefore, the difference in the gas adsorption between the two adsorption measurements is the strong gas adsorption amount.

Electrical Resistivity. Four-probe direct-current (DC) measurements were used to measure the electrical resistivities of the materials at room temperature (25 °C). Conductivity of the materials is obtained from the reciprocal of electrical resistivity. Samples were pressed into pellets with a diameter of 13 mm and thickness of 1 mm for measurements. Detailed information about sample preparation and four-probe DC electrical resistivity measurements can be found in the work of De Guzman.[35]

2.3 Catalytic Studies. The Na-2 × 3 tunnel structure manganese oxide was tested as a catalyst for indene oxidation. In a typical experiment, 10 mL of acetonitrile was first added into a 50-mL round flask as reaction media followed by an addition of 1 mmol of indene. A 50-mg portion of catalyst was then added to the flask followed by adding dropwise 1.5 mmol of *tertiary*-butyl hydroperoxide (TBHP). The reaction was conducted in an oil bath. Temperature was slowly increased from RT to 80 °C in about 4 h. Then the reaction was kept at 80 °C with stirring. A small amount of reaction mixture was taken from the reactor after 16, 24, and 40 h of reaction at 80 °C. The mixture was filtered with $MgSO_4$ before being analyzed with GC-MS.

3. Results and Discussion

3.1 Characterization. *Structure.* The XRD pattern of the prepared materials, as shown in Figure 1 a, is in good agreement with the standard pattern of natural 2

(32) Olivier, J. P. *J. Porous Mater.* **1995**, *2*, 9.
(33) Occelli, M. L.; Olivier, J. P.; Perdigon-Melon, J. A.; Auroux, A. *Langmuir* **2002**, *18*, 9816.
(34) Ravikovitch, P. I.; Haller, G. L.; Neimark, A. V. *Adv. Colloid Interface Sci.* **1998**, *76−77*, 203.
(35) De Guzman, R. N.; Awaluddin, A.; Shen, Y. F.; Tian, Z. R.; Suib, S. L.; Ching, S.; O'Young C. L. *Chem. Mater.* **1995**, 7, 1286.

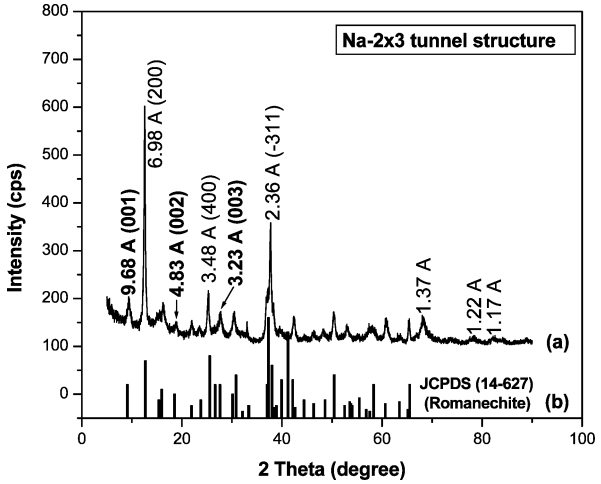

Figure 1. XRD pattern of the synthesized 2 × 3 tunnel structure manganese oxide. The column pattern (b) is the XRD pattern of natural romanechite (JCPDS file 14-627).

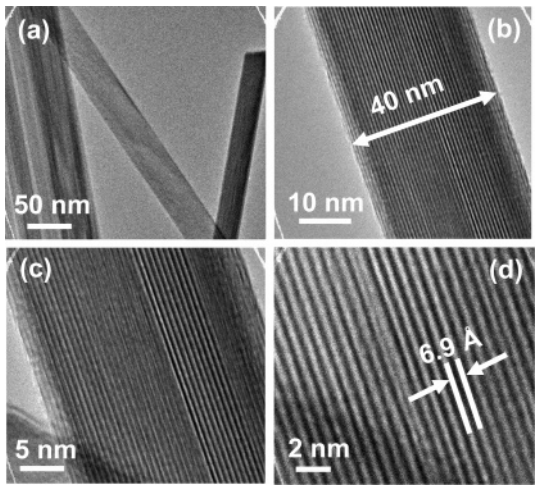

Figure 2. HRTEM images of the Na-2 × 3 tunnel structure manganese oxide. Lattice fringes of the (200) planes are clearly shown in (c) and (d).

× 3 tunnel structure manganese oxide, romanechite, Figure 1b. The characteristic diffraction peak for the (001) planes of romanechite is clearly observed at d = 9.68 Å ($2\theta \approx 9.2°$ for the Cu Kα source). No impurity phases were observed from the XRD pattern.

HRTEM pictures are shown in Figure 2. Increasing magnification from Figure 2a to d clearly reveals the lattice fringes of a fiber showing the lattice spacing of the (200) planes, $d \approx 6.9$ Å. No extra phases were observed on the fibers even down to the 2-nm scale.

Diffraction peaks at d spacing values of 9.7 and 7.0 Å, which correspond to the 3 MnO_6 unit side and the 2 MnO_6 unit side of the 2 × 3 tunnel, respectively, clearly prove the presence of the 2 × 3 tunnel structure. The good agreement of the XRD diffraction peak positions with natural romanechite suggests that the synthesized material has the same lattice structure as romanechite. The diffraction intensities of the peaks are not quite the same as those of romanechite which indicates that there are preferred orientations in the synthesized material. Because no extra XRD diffraction peaks were observed, this indicates that no hollandite, Mn_3O_4, or other impurities were present in the material. Therefore, the synthesized material is a pure 2 × 3 tunnel structure manganese oxide. This is also confirmed by the HRTEM measurements which show only nanofibers with a 2 × 3 tunnel structure without other phases growing with the fibers. Therefore, these results indicate that pure 2 × 3 tunnel structure manganese oxide can be successfully synthesized from hydrothermal treatment of Na-birnessite at neutral conditions. This synthetic 2 × 3 tunnel structure manganese oxide is referred to as OMS-6 herein.

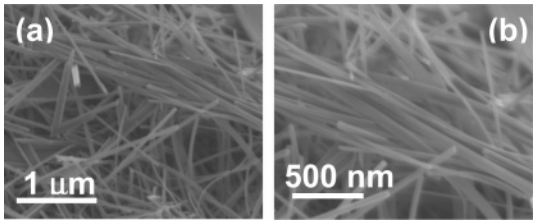

Figure 3. FESEM images of the Na-2 × 3 tunnel structure manganese oxide (OMS-6).

For many catalytic reactions, product selectivity may be greatly affected by the size of tunnels due to shape selectivity. Therefore, the different sizes of 2 × 3 tunnel other than the 2 × 2 or 3 × 3 tunnel may result in different catalytic activities and selectivities which will expand the application areas of manganese oxides. In addition, due to the successful reproduction of manganese oxides with 2 × 2 and 3 × 3 tunnel structures in laboratories, many potential applications have been explored in different areas such as (1) modification of their structures from doping and ion-exchanging for selective oxidation catalysis applications; (2) alteration of morphologies to obtain nanomaterials with higher surface areas; and (3) patterning of the tunnel structure semiconductors into more potentially functional materials. Therefore, the successful synthesis of 2 × 3 tunnel structure manganese will make modification of 2 × 3 tunnel structures or new morphologies possible. As a result, this introduces another new family of synthesized functional manganese oxide octahedral molecular sieve (OMS) materials.

Morphology. As shown in Figure 3, FESEM shows a homogeneous nanofibrous morphology of the Na-2 × 3 tunnel structure material. The fibers are a few micrometers long with an average diameter of about 40 nm. Only fibers/wires were observed for the products;, no plate morphology, which is a typical type of morphology for birnessite, was observed. This indicates the complete transformation of birnessite into the Na-2 × 3 tunnel structure within 2 d of hydrothermal treatment.

Thermal Stability. TGA analysis of the material under N_2 environments indicated that there are two major weight losses occurring at about 150 and 550 °C, as shown in Figure 4. About 3% of weight loss occurs below 200 °C and 10% of weight loss occurs from 200 to 700 °C.

TPD profiles of H_2O and O_2 elution from the 2 × 3 samples at elevated temperatures are shown in Figure 5A and B. One major H_2O desorption peak is observed from 50 to 180 °C centered at about 150 °C. Another H_2O elution peak can be observed starting from 250 °C and gradually ending at about 700 °C showing a tailing peak in the profile of Figure 5A. Integration of the peaks shows a peak area of 5.96×10^{-2} Torr·°C/mol tunnel for the first peak and an area of 3.31×10^{-2} Torr·°C/

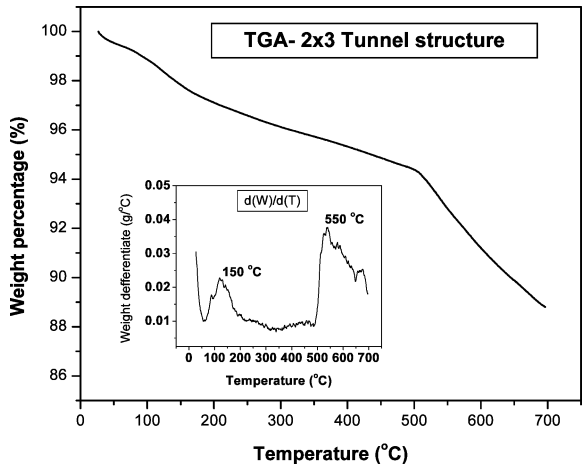

Figure 4. TGA measurements of the 2 × 3 tunnel structure manganese oxide. The inset is the differential analysis curve of the TGA curve showing two major weight losses at 150 and 550 °C.

mol tunnel for the second peak, the tailing peak. Profiles for O_2 elution are shown in Figure 5B. The first O_2 loss can be observed from the peak centered at about 150 °C. Then two elution peaks can be observed at 520 and 570 °C. These two peaks are not well deconvoluted, resulting in a broad peak centered at about 550 °C.

In situ XRD measurements of the 2 × 3 material under N_2 environments are shown in Figure 6A. At 150 °C (where adsorbed H_2O and O_2 will desorb from the material) diffraction from the (001) and (002) planes of the 2 × 3 tunnel structure, which correspond to the 2 × 3 tunnel side with three MnO_6 units ($d = 9.68$ Å) and the side with two MnO_6 units ($d = 6.98$ Å), respectively, is still preserved. A small change of diffraction at 2θ from 20 to 35° can also be observed after the material was heated at 150 °C. After the material is further heated at 550 °C under a N_2 flow, diffraction from the (001) planes and (200) planes starts to disappear; at the same time, some new peaks appear. A new phase corresponding to hausmannite, a spinel-like structure with a Mn_3O_4 stoichiometry, is produced.

Under an air flow or a UHP O_2 flow, even when the material was heated at 550 °C, the characteristic diffraction from the (100) planes and (002) planes of the 2 × 3 tunnel structure is still preserved, as shown in Figure 6B. Under an air flow, no peaks from phases other than the 2 × 3 tunnel structure are observed. While under a UHP O_2 flow, a small extra peak at 2θ of about 76.5° is observed, which might be due to diffraction from the (422) planes of hausmannite.

Both TGA and TPD measurements showed two major weight losses at about 150 and 550 °C in good agreement with each other. TPD measurements indicated that the weight loss at 150 °C is mainly due to H_2O and O_2. In situ XRD measurements suggest that under 150 °C, the 2 × 3 tunnel structure is still preserved because the reflections from the (001) planes ($d = 9.68$ Å), which correspond to the side of the 2 × 3 tunnel with 3 MnO_6 octahedra, and the (200) planes, which correspond to the side of the 2 × 3 tunnel with 2 MnO_6 octahedra, are preserved. Therefore, the loss of H_2O and O_2 under 150 °C should be due to desorption of physisorbed and chemisorbed H_2O and O_2. The weight loss at 550 °C is mainly due to loss of oxygen from the material as indicated from TPD measurements. At 550 °C under N_2 flow, the disappearance of the diffraction from the (001) and (200) planes indicated the loss of the 2 × 3 tunnel structure. Therefore, the loss of oxygen at 550 °C is mainly due to the loss of lattice oxygen which leads to the collapse of the 2 × 3 tunnel structure.

After collapse, the 2 × 3 tunnel structure is transformed into hausmannite (Mn_3O_4) with a spinel-like structure. This behavior is different from natural romanechite, which transforms to hollandite after being heated at 500 °C, as observed by Fleischer and Wadsley.[23,36] The reason for this difference is possibly due to the difference in types and amounts of tunnel cations which will produce different types or amounts of vacancies or defects under heating leading to different products after the tunnel collapses.

The preservation of the 2 × 3 tunnel at 550 °C under an air or a UHP O_2 flow indicates that the release of lattice oxygen can be suppressed by the presence of O_2 in the environment, which suggests that the material has a higher thermal stability in O_2 environments than in N_2 environments. The appearance of Mn_3O_4 at 550 °C in a UHP O_2 flow but not in an air flow may indicate that the presence of trace amounts of H_2O vapor in air can help to stabilize the tunnel structure.

Since the fibers grow in the same direction as the one-dimensional tunnel direction, the one-dimensional tunnel will be constructed by connecting each tunnel one by one along the fiber direction. Therefore, H_2O can only be eluted from the ends of the fibers. Elution of H_2O from the tunnels which are away from the ends of the fibers will be impeded from the H_2O molecules inside the tunnels which are close to the ends of the fibers. As

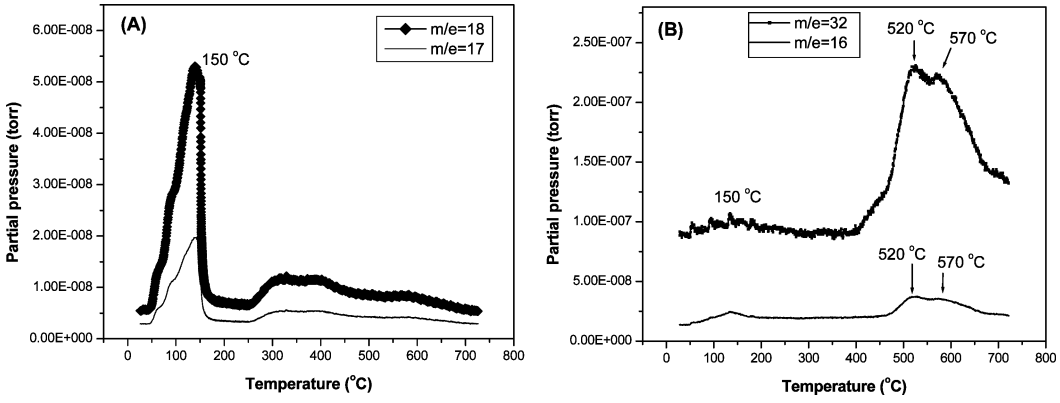

Figure 5. TPD profiles of (A) H_2O and (B) O_2 elution from the Na-2 × 3 tunnel structure manganese oxide from 26 to 726 °C.

Table 1. N_2 Physisorption Results for the 2 × 3 Tunnel Structure Manganese Oxide

BET surface area (m^2/g)	pore volume[a] (cm^3/g)	average pore size[b] (Å)	micropore size[c] (Å)	micropore area[d] (m^2/g)	% micropore area[e]
38 ± 0.17	0.21	209	7.5	2.8	7.4

[a] Single point of total pore volume at $P/P_0 = 0.995$. [b] By the BJH method. [c] By the DFT method (slit pore model). [d] By the *t*-plot method. [e] Percentage of micropore area.

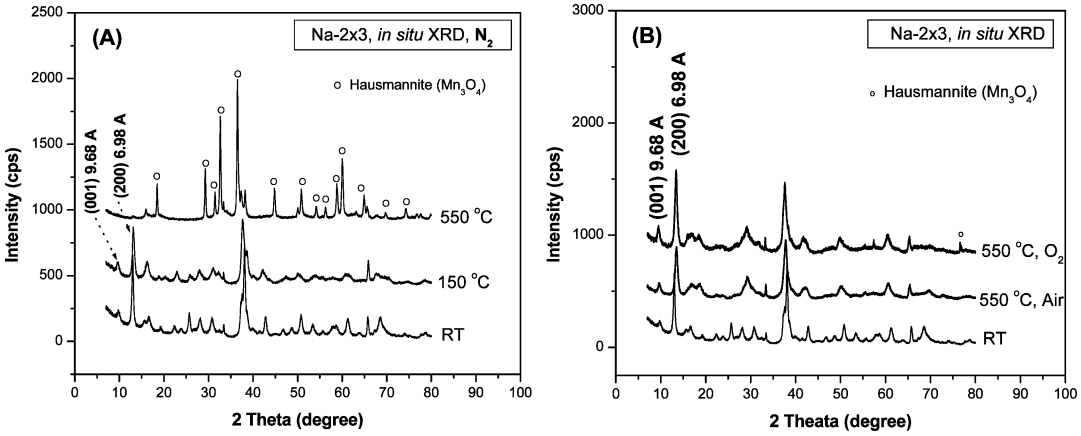

Figure 6. In situ XRD patterns of the Na-2 × 3 tunnel structure manganese oxide at elevated temperatures under (A) a N_2 flow and (B) an air and an O_2 flow.

a result, tunnel H_2O will be released sequentially and slowly from the center of the fibers to both ends of the fibers which will be characteristic with a tailing elution peak when the material is heated. The gradual loss of H_2O from 250 to about 700 °C observed in TPD profiles may indicate that this is due to the loss of tunnel H_2O.

Chemical Composition. AOS of framework manganese in the 2 × 3 tunnel structure manganese oxide is 3.84. The initial composition is $Na_{0.24}MnO_2 \cdot 0.71H_2O$ as determined by ICP−OES combined with the AOS results. However, the H_2O amount shown in the initial composition consists of both adsorbed and tunnel H_2O. To achieve information about hydrated H_2O in the tunnel, the results of TPD measurements can be used. The first elution peak ($m/e = 18$) in the H_2O profile in Figure 5 is assigned to desorption of adsorbed H_2O and the second peak is assigned to elution of tunnel H_2O. Therefore, from the total amount of H_2O in the material, the percentage of tunnel H_2O can be calculated from the ratio of the second peak area to the total area of the two peaks, which is about 35.7%. As a result, the composition of each 2 × 3 tunnel, without adsorption H_2O, is $(Na,H_2O)_2Mn_{12}O_{24}$ after rounding off all the numbers to integer values.

Surface Area and Porosity. N_2 physisorption shows a typical isotherm with hysteresis for porous materials, as shown in Figure 7. The inset in Figure 7 shows a broad mesopore and macropore size distribution calculated by the BJH method. The 2 × 3 tunnel structure manganese oxide has pores with diameters from 20 to 1000 Å showing a major pore size at around 850 Å. The results of surface area, pore volume, average pore size, and micropore surface area are summarized in Table 1. BET surface area of the material is about 38 m^2/g which is comparable to that of the hydrothermally synthesized 2 × 2 (OMS-2) and 3 × 3 (OMS-1) tunnel structure materials. An average pore size of about 209 Å was calculated by the BJH method. As determined

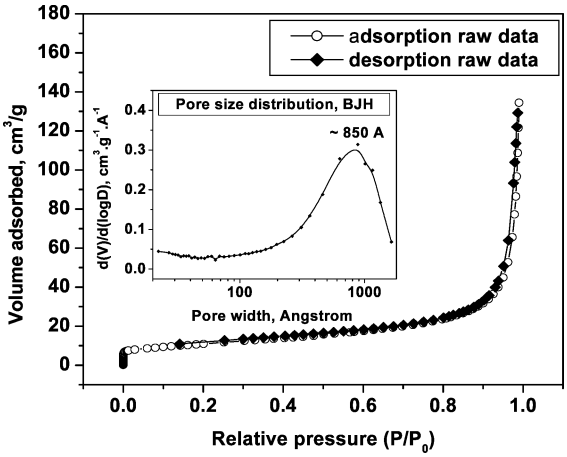

Figure 7. N_2 physisorption isotherms with the pore size distribution by the BJH method.

by the *t*-plot method, 7.4% of the surface area is contributed by micropores.

To apply the DFT method for extracting pore size distribution information, one needs to ensure that the model is valid and appropriate. The 2 × 3 tunnel has a slit-shape tunnel size, therefore using the NLDFT model based on slit-shape geometry is appropriate. Figure 8A shows a good fitting of experimental data to the model even in the low-pressure range ($P/P_0 = 10^{-6}$ to 10^{-2}). This confirms the validation of using the DFT method for extraction of the pore size distributions. The raw adsorption data shown in the inset of Figure 8A clearly indicates a significant adsorption of N_2 at relative pressures less than 10^{-3}. Figure 8B shows a significant amount of micropore volume in the materials with pore sizes less than 10 Å. Micropore size distribution calculated by the DFT method, as shown in Figure 8C, indicates a major micropore size of about 7.5 Å.

The surface energy is reported in terms of the effective Lennard−Jones interaction parameter (e) for the adsorptive−desorption pair divided by Boltzmann's constant (k). Therefore, the unit of the surface energy (e/k)

(36) Fleischer, M. *Am. Mineral.* **1960**, *45*, 177.

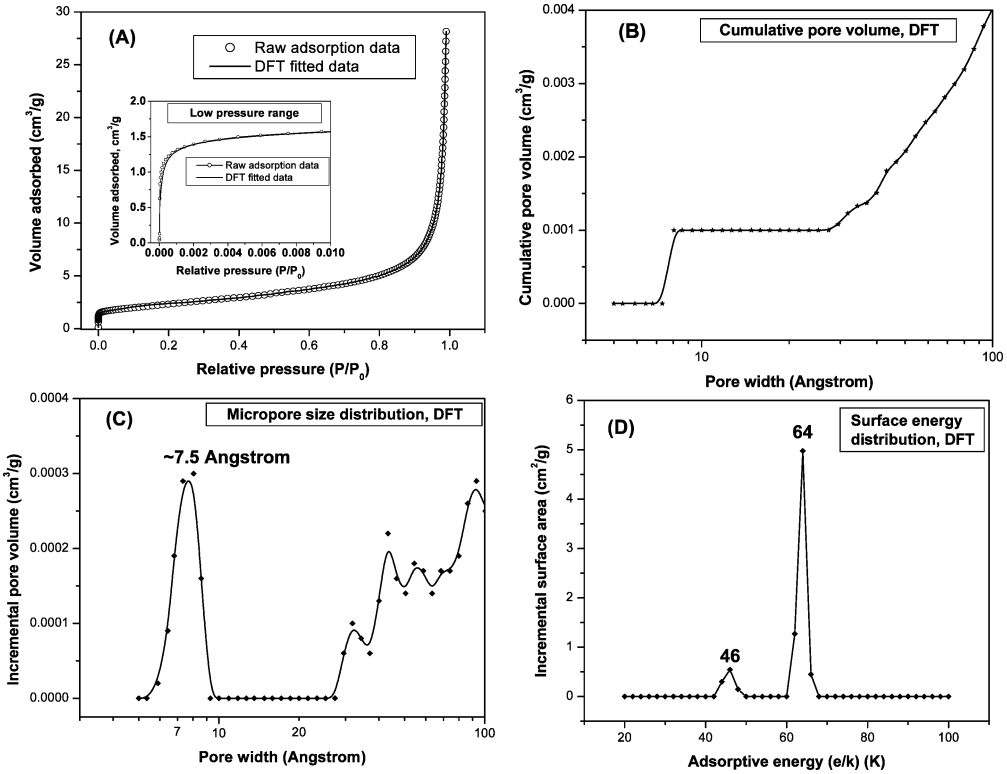

Figure 8. Results of data analyzed by the DFT method: (A) raw adsorption data and DFT fitted data; (B) distribution of cumulative pore volume with pore width; (C) distribution of incremental pore volume with pore width; and (D) adsorptive energy distribution.

is degrees Kelvin. Figure 8D shows the distribution of interaction energy (adsorptive energy) between N_2 molecules and the surface of the 2 × 3 tunnel structure manganese oxide. Two adsorptive energy maxima at 46 and 64 K are observed. The distribution of adsorptive energy can be used to evaluate the energetic heterogeneity of the sample surface. More adsorptive energy peaks will indicate a more energetically heterogeneous surface.

For pore size measurements, any adsorbed species in the materials, especially H_2O, will block the access of N_2 probe molecules into the pores leading to inaccurate assessments of porous structures. This blocking effect is more serious for micropores because they are so small (d < 2 nm) that the presence of H_2O molecules may completely block the pores. Therefore, before physisorption measurements, it is very important to remove the adsorbed/tunnel H_2O in the materials. As shown in the chemical composition result, the 2 × 3 tunnel structure has two H_2O molecules in each tunnel. TPD results show that these tunnel H_2O molecules start to elute from the 2 × 3 tunnel structure at a temperature of about 250 °C. Therefore, a degassing temperature of 300 °C was chosen to ensure the complete removal of any tunnel H_2O which might impede the adsorption of N_2 into the tunnels. In addition, to check if the nanoscale tunnel structures can be destroyed/collapsed after high-temperature degassing, the sample was analyzed by XRD right after the degassing. As shown in Figure 9, after 300 °C degassing, the 2 × 3 tunnel structure is still preserved because the characteristic (001) and (200) plane reflections are preserved. Another experiment showed that when the sample was degassed at 125 °C, the BET surface area of the material was about 35 m^2/g. This is not much different from the results (38 m^2/g)

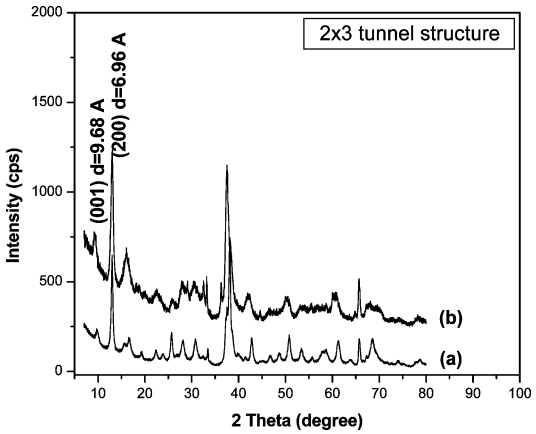

Figure 9. XRD patterns of OMS-6 (2 × 3 tunnel structure): (a) at room temperature; and (b) after degassing at 300 °C for 10 h.

when the sample was degassed at 300 °C. This indicates that degassing at 300 °C does not cause serious pore collapse or sintering to reduce surface area. Therefore, choosing the degas temperature at 300 °C can ensure that the pretreatments meet the pore size analysis requirements as follows: (1) removes the tunnel H_2O as completely as possible, (2) maintains the nanoscale tunnel structure, and (3) does not cause serious pore collapse or sintering.

Manganese oxides are the well-known porous OMS. The adsorption−desorption hysteresis confirmed that the 2 × 3 tunnel structure manganese oxide is a porous material. The apparent adsorption of N_2 at a relative pressure as low as 10^{-6} indicates that the material has micropores, which is also confirmed by the significant pore volume with pore widths less than 10 Å, as determined by the DFT method. The DFT method also

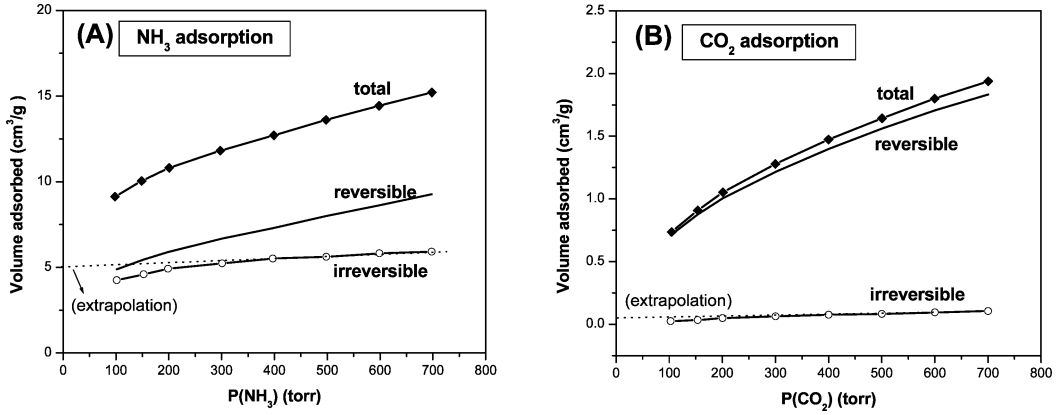

Figure 10. Measurements of acidic and basic sites in the 2 × 3 tunnel structure manganese oxide by (A) NH_3 chemisorption and (B) CO_2 chemisorption, respectively.

extracted an effective micropore size of about 7.5 Å for the 2 × 3 tunnel structure manganese oxide. The 2 × 3 tunnel structure has a tunnel size of 4.6 × 6.9 Å with a diagonal length of about 8.3 Å. Since there are two Na^+ ions present in each tunnel, as determined by ICP–OES, AOS titration, and TPD measurements, the accessible tunnel opening may be reduced from 8.3 Å. Therefore, the measured effective micropore size may be resulted from the accessible tunnel size. Since tunnels are connected along the fibers, with an obstacle effect from tunnel Na^+ ions, tunnels which are closer to both ends of the fibers are easier to access. Therefore, maybe only a small part of the tunnels is accessible for N_2 probe molecules. As a result, the measured surface area of the material is not high (38 m^2/g) compared to that of other microporous materials such as carbons.

NH_3 and CO_2 Chemisorption Measurements. Isotherms of NH_3 and CO_2 chemisorption on the Na-2 × 3 tunnel structure manganese oxide are shown in Figure 10. Extrapolation of the irreversible adsorption isotherms to zero pressure produces the strong chemisorption amounts of 5 cm^3 NH_3 and 0.05 cm^3 CO_2 on each gram of the sample. By assuming that each NH_3 or CO_2 molecule adsorbs on only one strong active site, the amount of strong acidic and basic sites on the 2 × 3 sample can be calculated to be 0.22 mmol/g sample and 0.002 mmol/g sample, respectively.

The framework manganese in romanechite is multivalent (3^+ and 4^+), as determined by Turner.[24] Therefore, two types of MnO_6 units will be present in the 2 × 3 tunnel structure manganese oxide, Mn(IV)O_6 and Mn(III)O_6. Since it is more negatively charged than Mn(IV)O_6, Mn(III)O_6 will have more chance to act as electron donors to form covalent bonds with CO_2 showing a Lewis basic activity. Whereas Mn(IV)O_6 may act as electron acceptors to form covalent bonds with NH_3 showing Lewis acidic activity. Therefore, Mn(IV)O_6 may be the major source for Lewis acidic sites and Mn(III)O_6 may be the major source for Lewis basic sites. Since AOS of the framework manganese in the Na-2 × 3 tunnel structure manganese oxide is 3.84, Mn(IV)O_6 is dominant compared to Mn(III)O_6 which results in more Lewis acidic sites in the material than Lewis basic sites. This may explain why there are much more measured strong acidic sides than strong basic sites.

Electrical Resistivity. Electrical resistivity of the Na-2 × 3 tunnel structure manganese oxide is 5.9 × 10^2 Ω·cm at 25 °C, as measured from a four-probe DC method. This corresponds to a conductivity of 1.7 × 10^{-3} $\Omega^{-1}\cdot cm^{-1}$.

Scheme 1. Possible Path for Indene Oxidation Catalyzed by OMS Materials

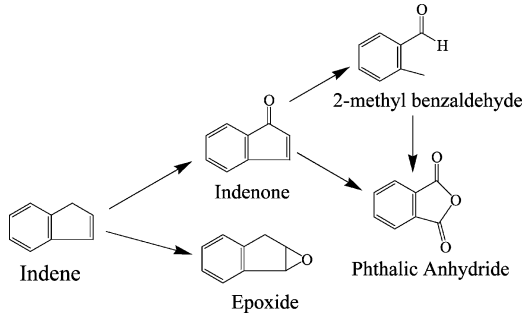

The electrical resistivity of the Na-2 × 3 tunnel structure manganese oxide (5.9 × 10^2 Ω·cm) is comparable to those of the OMS-2 (2 × 2 tunnel structure) materials, such as 4.4 × 10^2 Ω·cm for K-OMS-2 and 8.3 × 10^2 Ω·cm for Cu-OMS-2.[36] This electrical resistivity is much lower than that of OMS-1 (3 × 3 tunnel structure) materials (3.6 × 105 Ω·cm for Mg-OMS-1 and 1.6 × 10^5 Ω·cm for Cu-OMS-1).[35] This suggests that conductivity of the Na-2 × 3 tunnel structure manganese oxide is much higher than that of OMS-1 materials, which indicates that electrons are more localized in the Na-2 × 3 tunnel structure manganese oxide than in OMS-1 manganese oxides. As pointed out by many researchers, natural and synthetic manganese oxides usually have cation vacancies to affect their local structures and electron transport properties.[37–39] The relative high conductivity of 2 × 3 tunnel structure may suggest that more cation vacancies are present in the Na-2 × 3 tunnel structure than in OMS-1 materials. As a result, the 2 × 3 tunnel structure may show higher catalytic activity for reactions involving cation or electron transport.

3.2 Catalytic Studies. Indene oxidation catalyzed by OMS manganese materials is proposed to follow the mechanism in Scheme 1.[40] Indene can be directly oxidized to epoxide or to phthalic anhydride via inter-

(37) Post, J. E.; Von Dreele, R. B.; Buseck, P. *Acta Crystallogr.* **1982**, *38*, 1056.
(38) Kaczmarek, J.; Wolska, E. *J. Solid State Chem.* **1993**, *103*, 387.
(39) Boix, T.; Sapina, F.; El-Fadli Z.; Martinez E.; Beltran, A. *Chem. Mater.* **1998**, *10*, 1569.
(40) Son, Y.-C. Ph.D. Thesis, The University of Connecticut, 2003.

Table 2. Results of Indene Oxidation Catalyzed by the Synthesized 2 × 3 Tunnel Structure Manganese Oxide

		selectivity			
sample	conversion	epoxide	phthalic anhydride	indenone	2-methyl-benzadehyde
Na-2 × 3 (16 h)	70%	3%	42%	35%	20%
Na-2 × 3 (24 h)	80%	6%	51%	33%	10%
Na-2 × 3 (40 h)	96%	7%	73%	13%	7%
K-OMS-2 (24 h)[a]	10%	70%	ND[b]	21%	9%
Fe−K-OMS-2 (24 h)[a]	45%	96%	ND	3%	1%
Co-OMS-1 (24 h)[a]	75%	7%	60%	20%	13%
Fe-OMS-1 (24 h)[a]	70%	1%	57%	29%	13%

[a] Reference data from ref 40. [b] ND= not detected.

mediates indenone or 2-methyl-benzaldehyde, respectively. Reaction results are included with the reference data in Table 2. With increasing reaction time from 16 to 40 h, the conversion of indene is increased from 70% to 96% and the selectivity of epoxide is increased from 3% to 7%. The product is dominant with phthalic anhydride showing a selectivity of 42% and 73% for 16 and 40 h reaction, respectively. For a 24-h reaction, the 2 × 2 tunnel structure manganese oxides did not show any selectivity for phthalic anhydride, whereas the 2 × 3 and 3 × 3 tunnel structures show a comparable selectivity of around 50−60% for phthalic anhydride.

Increase of conversion and selectivities toward epoxide and phthalic anhydride with reaction time indicates that the reaction has not reached kinetic equilibrium. For a 40-h reaction, even when the conversion is 96%, there are still 20% of intermediates which were not oxidized to phthalic anhydride. This may indicate a complete consumption of the oxidant, TBHP. Therefore, a semi-batch reactor with step addition of TBHP or a CSTR reactor may be used to increase the selectivity for phthalic anhydride. Compared with the 2 × 2 tunnel structure, the 2 × 3 and 3 × 3 tunnel structure manganese oxides show a higher selectivity toward phthalic anhydride. This may be related to the size of the tunnel which will cause different shape selectivities. As shown by Makwana, framework oxygen in the OMS-2 materials plays a critical role for selective oxidation of benzyl alcohol.[41] Cation vacancies, which can change electronic properties of the structure, may also change catalytic activity. Materials with more cation vacancies may show higher catalytic activity for the oxidation reactions because there will be more active sites in the material for electron transfer (reduction/oxidation). Therefore, many factors such as tunnel size, cation vacancies, framework oxygen, oxygen vacancies, AOS, and surface area many combine together to control the catalysis of indene oxidation by the 2 × 3 tunnel structure (OMS-6).

The application of indene oxidation is an example to demonstrate that the synthetic 2 × 3 tunnel structure manganese oxide has catalytic effects on organic oxidations. Studies have showed that the 2 × 2 tunnel structure manganese oxide (OMS-2) is a good catalyst for low-temperature CO oxidation,[42] total oxidation of volatile organic compounds (VOCs),[43] propanol decomposition,[44] benzyl alcohol oxidation,[41] and olefin epoxidation.[45] The 2 × 3 tunnel structure manganese oxide has a structure similar to that of the 2 × 2 tunnel structure. Therefore, applications of the synthetic 2 × 3 tunnel structure as a catalyst for these reactions are also possible.

Conclusions

Manganese oxide with a 2 × 3 tunnel structure as natural romanechite has been successfully synthesized in the laboratory using Na^+ or hydrated Na^+ ions as the structure director from hydrothermal treatment of Na-birnessite at 200−250 °C for 2 d. No impurity phases were observed in the synthetic Na-2 × 3 tunnel structure manganese oxide. The material is nanofibrous with an average fiber diameter of about 40 nm and an electrical resistivity of 5.9×10^2 Ω·cm which is comparable to that of OMS-2 manganese oxides but much lower than that of OMS-1 manganese oxides. The material has micropores with a major pore width of 7.5 Å. Under N_2 environments, the Na-2 × 3 tunnel structure is stable below 550 °C and transforms into hausmannite at 550 °C or higher temperatures. Under O_2 environments, the Na-2 × 3 tunnel structure is stable at 550 °C. The synthetic Na-2 × 3 tunnel structure manganese oxide shows promising catalytic activities for the synthesis of phthalic anhydride from indene oxidation.

Acknowledgment. We thank the Geosciences and Biosciences Division, Office of Basic Energy Sciences, Office of Science, U.S. Department of Energy for financial support. We also thank Dr. Jonathan Hanson, Dr. Xianqin Wang, and Dr. Francis S. Galasso for the helpful discussions.

CM049291R

(41) Makwana, V. D.; Son, Y.-C.; Howell, A. R.; Suib. S. L. *J. Catal.* **2002**, *210*, 46.

(42) Xia, G.-G.; Yin, Y. G.; Willis, W. S.; Wang, J. Y.; Suib, S. L. *J. Catal.* **1999**, *185*, 91.

(43) Luo, J.; Zhang, Q.; Huang, A.; Suib, S. L. *Microporous Mesoporous Mater.* **2000**, *35−36*, 209.

(44) Chen, X.; Shen, Y.-F.; Suib, S. L.; O'Young C. L. *J. Catal.* **2001**, *197*, 292.

(45) Ghosh, R.; Son, Y.-C.; Suib, S. L. *J. Catal.* **2004**, *224*, 288.